

# Topology of large scale structure as test of modified gravity

Xin Wang,<sup>1,2</sup> Xuelei Chen,<sup>1,3</sup> and Changbom Park<sup>4</sup>

<sup>1</sup>*Key Laboratory of Optical Astronomy, National Astronomical Observatories,  
Chinese Academy of Sciences, Beijing, 100012, China*

<sup>2</sup>*Graduate School of Chinese Academy of Sciences, Beijing 100049, China*

<sup>3</sup>*Center of High Energy Physics, Peking University, Beijing 100871, China*

<sup>4</sup>*Korea Institute for Advanced Study, Dongdaemun-gu, Seoul 130-722, Korea*

The genus of the iso-density contours is a robust measure of the topology of large scale structure, and it is relatively insensitive to nonlinear gravitational evolution, galaxy bias and redshift-space distortion. We show that the growth of density fluctuations is scale-dependent even in the linear regime in some modified gravity theories, which opens a possibility of testing the theories observationally. We propose to use the genus of the iso-density contours, an intrinsic measure of the topology of large-scale structure, as a statistic to be used in such tests. In Einstein's general theory of relativity, density fluctuations are growing at the same rate on all scales in the linear regime, and the genus per comoving volume is almost conserved as structures are growing homologously, so we expect that the genus-smoothing scale relation is basically time-independent. However, in modified gravity models where structures grow with different rates on different scales, the genus-smoothing scale relation should change over time. This can be used to test the gravity models on large scales. We studied the case of the  $f(\mathcal{R})$  theory, DGP braneworld theory as well as the parameterized post-Friedmann (PPF) models. We also forecast how the modified gravity models can be constrained with optical/IR or 21cm surveys in the near future.

## I. INTRODUCTION

The large scale structure has long been a major source of information on cosmic evolution. The most frequently used statistics of the large scale structure, such as the two-point correlation function and the density power spectrum, and especially the baryon acoustic oscillation (BAO) signatures in the power spectrum have been widely used in tests of cosmological models and precisional measurements of cosmological parameters [1–3]. However, these two-point statistics do not exhaust all of the information content about the large scale structure—at least not in the non-gaussian case. There are also some limitations on the application of these statistics. As the perturbations grow larger, their evolution becomes nonlinear, resulting in a distorted power spectrum and the emergence of gravity-induced non-gaussianity. This has a crucial influence in the extraction of the absolute BAO scale: at  $k = 0.1 \sim 0.15 \text{Mpc}/h$  where the first BAO peak is located, the non-linear evolution of the power spectrum amounts to 2% to 5% differences between  $z = 0$  and  $z = 0.5$  [4]. Accurately modeling the non-linear evolution is highly non-trivial, and practical application in actual model test/parameter determination also requires fast and easy-to-implement algorithm. Although progresses have been made in more sophisticated perturbative expansion [5–10] or reconstruction [11, 12] procedures to correct for the effect of non-linear evolution, a precise yet practical method to take into account of these effects has yet to be developed. Other systematic effects, such as the clustering bias and the redshift distortion could also affect the outcome of the measurement. Such effects may significantly limit the accuracy of cosmological tests for future redshift surveys, where the statistical error on the BAO scale would be at the one percent level.

An alternative approach to the correlation function and power spectrum is the topology of the iso-density contours, in particular the genus of these contours. This offers another way to characterize the statistical property of the large-scale structure, and is insensitive to the systematic effects discussed above, since the intrinsic topology does not change as the structures form, at least not until the iso-density contours eventually break at shell crossing [13, 14]. This provides a robust statistic for cosmology. Compared with the power spectrum, the genus changes only by 0.5% between  $z = 0.5$  and  $z = 0$  [15]. This is particularly true when using the volume fraction for the threshold levels to identify the contours. According to the second order perturbation theory [16], there is no change in the genus at median density threshold due to weak nonlinear evolution, because the iso-density contours enclosing a given fraction of volume do not change as long as the gravitational evolution conserves the rank ordering of the density. Similarly, a monotonic clustering bias does not result in any difference in the iso-density contours, and a continuous coordinate mapping into redshift space does not affect the genus statistics either. In  $\Lambda\text{CDM}$  model with general relativity, the genus is conserved during the different epochs in the linear regime of evolution. Therefore, by observing the genus curve at the different redshifts and smoothing scales, one can use it as a robust standard ruler for cosmological measurements [14].

In the present paper, we consider the phenomenological consequences of alternative gravity theories. A number of such models, e.g. the  $f(\mathcal{R})$  theory [17–20] and the DGP brane-world model [21], have been proposed to explain the accelerated expansion of the Universe. Unlike the general relativity, where the growth of the density fluctuation is at

the same rate on all scales during the linear evolution, the modified large-scale gravitational forces induced by extra scalar field can in general introduce new scale dependence in the growth of structure, and therefore distort the genus curve in a time-dependent way. This provides us a new tool for distinguishing GR from its various alternatives, which probe the combined effects of background expansion and the growth of the structures, and therefore is able to break the degeneracy between the dark energy and modified gravity models from expansion data alone [22, 23]. Furthermore, such measurement also has the advantage that it is insensitive to nonlinear systematics. This is particularly useful because for some modified gravity models, such as the ones invoking the chameleon [24, 25] mechanism or the Vainshtein mechanisms [26, 27], it is non-trivial to treat the effect of nonlinear evolution on the power spectrum. The genus, on the other hand, is almost conserved during much of the evolution, thus allowing us to avoid dealing with such problems in the nonlinear regime. Instead, we may make the calculation in the linear regime, and expect it to be almost unchanged until very late into the nonlinear regime.

Below in Sec.II we briefly review the calculation of the genus density and the cosmological perturbation theory in the parametrised post-Friedmann framework. In Sec.III we discuss how the genus density changes in the various modified gravity models. We forecast the prospects of observation with the future redshift surveys in Sec. IV and conclude in Sec. V. An estimate of statistical uncertainty of the genus measurement is given in the Appendix.

## II. THEORY

The genus density  $\mathcal{G}$  is given by the genus, i.e. (the number of holes - number of isolated regions) divided by the volume  $V$ . Smoothing the tracer distribution by a Gaussian filter with scale  $R_G$ , then the iso-density contours of smoothed field can be identified for a given variance-normalized density threshold  $\nu \equiv \delta/\sigma(R_G)$  or volume fraction. The genus curve, i.e. the genus per unit volume of the iso-density contours as a function of such threshold, could be measured.

In the particular case of gaussian fluctuations, the genus curve can actually be calculated analytically [29, 30]:

$$\mathcal{G}(\nu) = \mathcal{A}(1 - \nu^2)e^{-\nu^2/2}, \quad (1)$$

and the amplitude  $\mathcal{A}$  is

$$\mathcal{A} = \frac{1}{4\pi^2 3^{3/2}} \left( \frac{\int d^3k k^2 P(k)W(kR_G)}{\int d^3k P(k)W(kR_G)} \right)^{3/2}. \quad (2)$$

where  $W$  is the window function for smoothing. The threshold level  $\nu$  is related to the volume fraction  $f$  on the high-density side of the density contour surface via

$$f = \frac{1}{\sqrt{2\pi}} \int_{\nu}^{\infty} e^{-x^2/2} dx \quad (3)$$

For non-gaussian primordial fluctuations, the perturbative formula for the genus curve has also been derived [31], though we will not consider this more general case in the present paper. As the structures grow, the fluctuations would become non-gaussian gradually, and the genus is no longer solely determined from the nonlinear power spectrum of the structure. However, as shown in [16], the amplitude of the genus curve does not change up to second order perturbation in the weak non-linear regime, because the genus is a topological indicator which is independent of simple growth of clustering without merger. Therefore, the genus is a quantity which is better conserved than the shape of the power spectrum during quasi-linear evolution, and the one derived from the linear power spectrum could be used.

As demonstrated by [14], when the correct redshift-distance relationship  $r(z)$  is adopted, one would be using the same comoving volume  $V(z) = (D_A^2/H)(z)$  and smoothing scale  $R_G$  at different epochs. Here  $D_A(z)$  is the angular diameter distance and  $H(z)$  is the Hubble expansion rate. Therefore the data at different redshifts actually enclose statistically almost the same amount of structures, and the amplitude of genus curve  $\mathcal{A}$  would be almost the same at different redshifts. This can also be seen from Eq. (2), which shows that  $\mathcal{A}$  actually measure the slope of the power spectrum around the smoothing scale  $R_G$ . Since in the linear regime of GR only the growth rate of the structure, not the shape of it, evolves,  $\mathcal{A}$  would be conserved. However, if an incorrect  $r(z)$  due to an incorrect cosmology is adopted, both  $V(z)$  and  $R_G$  would be mis-estimated. Since the topology of the structure is not scale-free, the genus enclosed in a wrongly sized volume and smoothed with a wrong scale would lead to deviation from the actual one, in this case

$$\mathcal{A}_Y(z, R_{G,Y})R_{G,Y}^3 = \mathcal{A}_X(R_{G,X})R_{G,X}^3, \quad (4)$$

where  $Y$  is the adopted cosmology parameters while  $X$  is the true cosmology. The smoothing scale  $R_G$  for different cosmologies are related to each other by

$$(R_{G,X}/R_{G,Y})^3 = (D_A^2/H)_X/(D_A^2/H)_Y, \quad (5)$$

Utilizing this effect, topology of the large scale structure can serve as a standard ruler in cosmology.

Since the genus would be affected by modifying the density perturbation through Eq. (2), we now consider the evolution of density perturbations in modified gravity. A wide range of modified gravity theories which satisfy the basic requirement of being a metric theory where energy-momentum is covariantly conserved, can be studied in the so called parametrized post-Friedmann (PPF) framework [32]. For these theories, on superhorizon scales structure evolution must be compatible with background evolution, on intermediate scales the theory behaves as a scalar-tensor theory with a modified Poisson equation, while on small scales, to pass stringent local tests, the additional scalar degree of freedom must be suppressed. The evolution of linear perturbations in theories which satisfy these conditions can be characterized by a few parameters. With the Newtonian gauge temporal and spatial curvature scalar perturbation  $\Psi$  and  $\Phi$ , we introduce

$$g \equiv \frac{\Phi + \Psi}{\Phi - \Psi}, \quad \Phi_- \equiv \frac{\Phi - \Psi}{2}. \quad (6)$$

In the absence of anisotropic stress,  $\Phi = -\Psi$ , and  $g = 0$  for the GR case. However, in modified gravity  $g$  may not be zero. From causality considerations, on superhorizon scales the evolution of metric perturbation must be determined entirely by the expansion rate and  $g$  to the first order of  $k_H$ , with

$$\lim_{k_H \rightarrow 0} \left( \Phi'' - \Psi' - \frac{H''}{H'} - \left( \frac{H'}{H} - \frac{H''}{H'} \right) \Psi \right) = \mathcal{O}(k_H^2) = \frac{1}{3} f_\zeta k_H V_m. \quad (7)$$

where  $' \equiv d/d \ln a$ ,  $V_m \sim k_H$  is the velocity perturbation,  $k_H = k/Ha$ . However, to the next order, we can then introduce  $f_\zeta$  to characterize the curvature perturbation on superhorizon scales. The subscript  $\zeta \equiv \Phi - V_m/k_H$ , which is the curvature perturbation in matter comoving gauge, indicates the fact that the LHS of Eq. (7) equals to  $\zeta$  in the matter comoving gauge. On subhorizon scales, the lensing potential satisfies the modified Poisson equation,

$$k^2 \Phi_- = \frac{4\pi G}{1 + f_G} a^2 \rho_m \Delta_m(k), \quad (8)$$

where  $\Delta_m$  is the fractional density perturbation,  $f_G$  parametrizes modification to Newton constant. Equivalently, we can introduce a new scalar field  $\varphi$  which characterise the extra source felt by nonrelativistic particles,

$$-k^2 \Psi(k) = \frac{4\pi G}{1 + f_G} a^2 \rho_m \Delta_m(k) + \frac{1}{2} k^2 \varphi(k), \quad (9)$$

where  $\varphi(k)$  satisfies the equation

$$-k^2 \varphi(k) = \frac{8\pi G}{1 + f_G} a^2 g(a, k) \rho_m \Delta_m(k). \quad (10)$$

Thus in the subhorizon regime, the scale-dependent deviation from the GR is described by  $\varphi(k)$ . In summary, in the PPF parameterization, the modified gravity model is characterized by  $g(a, k)$ ,  $f_G(a)$ ,  $f_\zeta(a)$  and the superhorizon-subhorizon transition scale  $c_\Gamma$ . The evolution of these functions depends on the specific model. The fluctuation power spectrum for such theories can be calculated by using the public Boltzmann code `camb` with the PPF module<sup>1</sup> [33–35].

### III. MODELS

As a first example we consider the  $f(\mathcal{R})$  theory,

$$S = \int d^4x \sqrt{-g} \left[ \frac{\mathcal{R} + f(\mathcal{R})}{16\pi G} + \mathcal{L}_m \right], \quad (11)$$

---

<sup>1</sup> <http://camb.info/ppf/>

where  $\mathcal{R}$  is the Ricci scalar and  $\mathcal{L}_m$  is the matter Lagrangian density. For a given expansion history  $H(a)$ , e.g. the effective dark energy equation of state  $w_e = -1$ , in order to explain the late-time acceleration, the form of  $f(\mathcal{R})$  can be determined from a second order differential equation

$$-f_{\mathcal{R}}(HH' + H^2) + \frac{1}{6}f + H^2 f_{\mathcal{R}\mathcal{R}}\mathcal{R}' = \frac{8\pi G}{3}\rho - H^2, \quad (12)$$

where  $\rho$  is the total energy density,  $f_{\mathcal{R}}$  and  $f_{\mathcal{R}\mathcal{R}}$  are the first and second derivatives of  $f(\mathcal{R})$  with respect to  $\mathcal{R}$ . A given expansion history permits a family of  $f(\mathcal{R})$  functions, the additional degree of freedom is usually characterized by  $B_0$ , the present day value of the function  $B(a)$ , which is the square of the Compton scale given by

$$B(a) \equiv \frac{f_{\mathcal{R}\mathcal{R}}\mathcal{R}'\frac{H}{H'}}{1 + f_{\mathcal{R}}} \quad (13)$$

$B_0$  is thus a model parameter of the  $f(\mathcal{R})$  theory, which is to be constrained by structure growth. Given  $H(a)$  and  $B(a)$ , the metric ratio at superhorizon scale  $g_{SH}$  can be obtained by solving the differential equation

$$\Phi'' + \left(1 - \frac{H''}{H'} + \frac{B'}{1-B} + B\frac{H'}{H}\right)\Phi' + \left(\frac{H'}{H} - \frac{H''}{H'} + \frac{B'}{1-B}\right)\Phi = 0, \quad (14)$$

and utilizing the relation  $\Psi = (-\Phi - B\Phi')/(1 - B)$ . As shown by [32], the scale dependent  $g(a, k)$  can be well fitted by the interpolation function

$$g(a, k) = \frac{g_{SH} + g_{QS}(c_g k_H)^{n_g}}{1 + (c_g k_H)^{n_g}}. \quad (15)$$

where  $g_{QS} = -1/3$ ,  $c_g = 0.71B^{1/2}$  and  $n_g = 2$ , with other PPF parameters  $f_{\zeta} = -1/3g$ ,  $f_G = f_{\mathcal{R}}$  and  $c_{\Gamma} = 1$ .

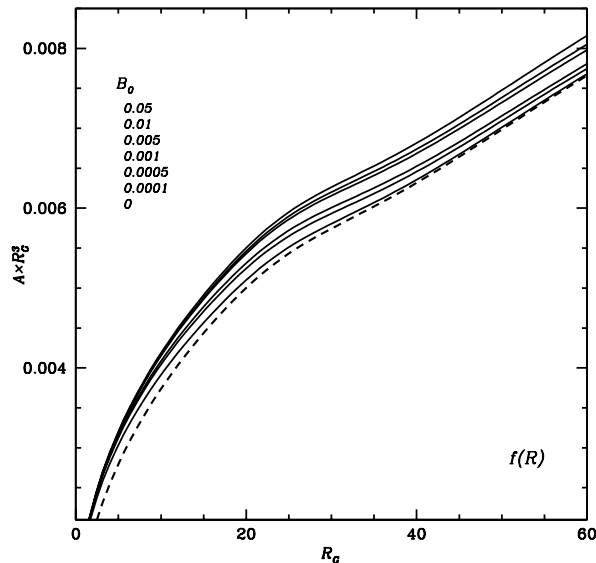


FIG. 1: The genus per smoothing volume as a function of smoothing scale  $R_G$  at  $a = 1$  for  $f(\mathcal{R})$  theories with different  $B_0$ .

Given PPF parameters of  $f(\mathcal{R})$  theory above, especially  $g(a, k)$ , the matter power spectrum at relevant scales can be obtained with the help of Eq. (9, 10). In Fig. (1), we plot the genus amplitude of the genus as a function of the smoothing scale  $R_G$  at  $a = 1$  for several  $f(\mathcal{R})$  models characterised by different  $B_0$  values. For models with greater  $B_0$  value, the genus is larger.

We may also see how the amplitude of the genus curve varies as a function of redshift. In Fig. (2), we plot the redshift evolution of  $\mathcal{A}$  for a fixed smoothing scale  $R_G = 15\text{Mpc}/h$ . Compared with the horizontal line, which corresponds to GR in the bottom of the figure, the amplitude of the genus curve exhibits a strong time dependence for the  $f(\mathcal{R})$  theory with a total variation of about 10% for  $B_0 \gtrsim 0.01$ .

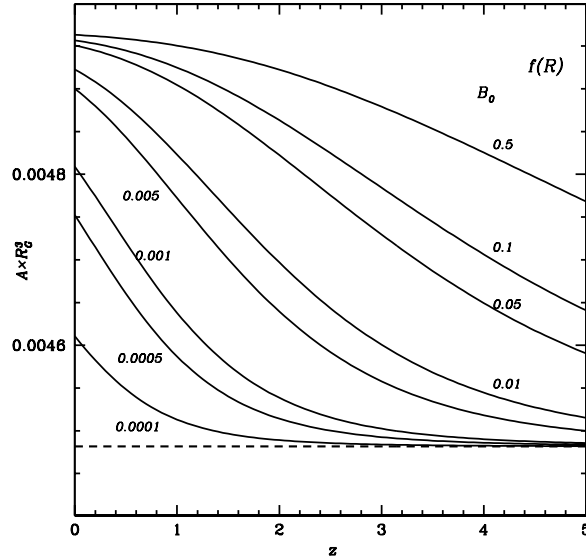


FIG. 2: The redshift evolution of genus amplitude for  $f(\mathcal{R})$  theories with different  $B_0$ .

From these figures it is obvious that for larger  $B_0$ , the deviation from GR is greater, i.e. the variation of the genus is stronger in the  $f(\mathcal{R})$  theory. By inspecting the perturbative variables in detail, with other PPF parameters we find that this is mainly due to the monotonically increasing deviation of  $\Phi_-$  from the GR prediction with respect to the wavenumber  $k$ . The extra scalar degree of freedom  $\varphi = -f_{\mathcal{R}}$  enhances the gravitational force at smaller scales, and therefore increase the slope of the clustering.

Next we consider the self-accelerating Dvali-Gabadadze-Porrati (DGP) braneworld model. In this model, our universe is a (3+1) dimensional brane embedded in an infinite Minkowski bulk, it can be described by the following action

$$S = \int d^5x \sqrt{-g_{(5)}} \left[ \frac{\mathcal{R}_{(5)}}{16\pi G_{(5)}} + \delta(\chi) \left( \frac{\mathcal{R}_{(4)}}{16\pi G_{(4)}} + \mathcal{L}_m \right) \right], \quad (16)$$

where  $\mathcal{R}_{(i)}, G_{(i)}$ ,  $i = 4, 5$  is the Ricci scalar and Newton constant in the brane and the bulk respectively. At the background level, [21] showed that the consequent Friedmann equation

$$H^2(a) = \left( \sqrt{\frac{8\pi G_{(4)}}{3} \sum_i \rho_i + \frac{1}{4r_c^2} + \frac{1}{2r_c}} \right)^2 - \frac{K}{a^2}, \quad (17)$$

leads to a de-Sitter phase at late time characterized by the crossover scale  $r_c = G_{(5)}/2G_{(4)}$ .

Above the horizon, the evolution of the perturbation can be solved by iterative scaling method [36], and the metric ratio  $g_{SH}$  is well fitted by function

$$g_{SH}(a) = \frac{9}{8Hr_c - 1} \left( 1 + \frac{0.51}{Hr_c - 1.08} \right). \quad (18)$$

In the quasi-static regime,

$$g_{QS}(a) = -\frac{1}{3} \left[ 1 - 2Hr_c \left( 1 + \frac{1}{3} \frac{H'}{H} \right) \right]^{-1}. \quad (19)$$

Thus the scale dependent  $g(a, k)$  can be described by the same interpolation equation Eq. (15) with  $c_g = 0.4$ ,  $n_g = 3$ . Other PPF parameters are  $f_\zeta = 0.4g$ ,  $f_G = 0$ ,  $c_\Gamma = 1$ .

From the calculation, we find that the major scale-dependent modification to the growth of the structure is in the superhorizon regime ( $k/aH \ll 1$ ). With a Gaussian smoothing scale of 15Mpc/h, only about 0.07% deviation of  $\mathcal{A}$

are found compared with GR, which can hardly be distinguished by the observation in the near future. In this case other techniques such as the ISW effect or the growth rate are more viable. However it should also be noticed that [37, 38], with the help of Vainshtein mechanism which bring the gravity back into GR at small scales, the nonlinear evolution can also induce significant scale-dependent deviations at relevant scales. We leave this topic to our further study.

At last we consider more generic models in the context of PPF. We note that amongst the PPF variables,  $f_G(a)$  and  $f_\zeta(a)$  connect the metric fluctuations to the matter fields and are only functions of time. Rescaling the amplitude of the matter fluctuations without changing the shape (i.e. slope) of the power spectrum would not affect the genus, so here we do not need to consider them, as the topological measurements would be insensitive to these. Similarly, for the wavenumber range corresponding to smoothing scale of the order  $\mathcal{O}(10)\text{Mpc}/h$  relevant to large-scale genus topology study, the mode is in the sub-horizon regime, so the variable  $g_{SH}$  which describes the modification to the superhorizon metric can also be excluded from our consideration.

Following [39], we adopt the scale dependent  $g$  as an interpolation function between the super-horizon regime  $g_{SH}$  and the quasi-static regime  $g_{QS}$  (c.f. Eq. (15)). Both  $c_g(a)$  and the power index  $n_g$  can affect the behavior of the transition between the two regimes.

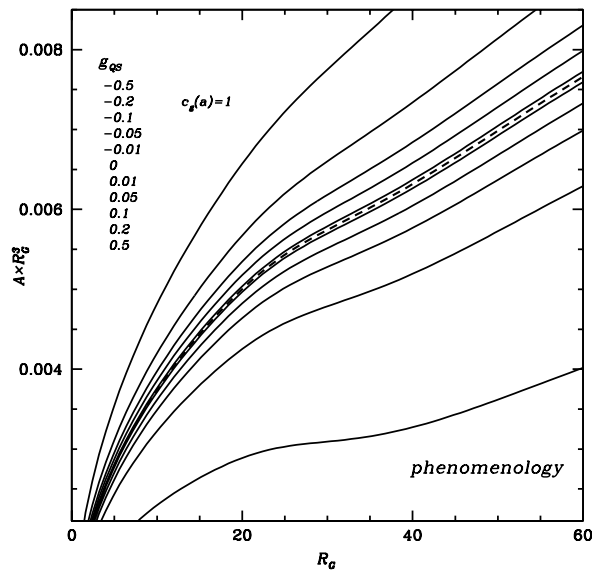


FIG. 3: The genus per smoothing volume as a function of smoothing scale  $R_G$  at  $a = 1$  for the phenomenological model of different  $g_{QS}$  with  $c_g(a) = 1$ .

Eq. (15) shows that for each Fourier mode the time-dependent factor  $c_g k_H = c_g k / (aH)$  determines the moment and scale at which the gravity deviate from the GR case. In this simple model,  $\lim_{k \rightarrow 0} g(a, k) = 0$ , therefore  $\varphi$  would be modified when  $k \geq k_t = (aH)/c_g$ .

First let us consider the case where  $c_g$  is a constant. The transition scale would first slowly decrease as  $k_t \sim a^{-1/2}$  during the matter dominated era, then start to increase during the era of accelerated expansion. In order to get significant effect on scales of  $k \sim \mathcal{O}(0.1)h/\text{Mpc}$  or above,  $c_g$  should be at least larger than  $(aH)/k$ , which is about  $\mathcal{O}(0.01)$ .

As an example, in Fig. (3), we plot the genus per smoothing volume as a function of  $R_G$  for various  $g_{QS}$ , while keeping  $g_{SH} = 0$ ,  $c_g(a) = 1$ , and  $n_g = 2$ . Compared with the GR case (i.e.  $g_{QS} = 0$ ), the difference is quite apparent. At any time, the metric deviation Eq. (15) is a monotonic function of the wavenumber, this induce the same monotonicity in the deviation of  $\Phi_-$  from GR. Specifically, negative value of  $g_{QS}$  and therefore the positive extra force  $-\nabla\varphi$ , will increase  $\Phi_-$  as well as the slope of power spectrum at  $k \gtrsim k_t$ , and ultimately rise the value of the genus. On the other hand, positive  $g_{QS}$  behaves in the opposite way. Nevertheless, owing to the slow evolution of  $k_t$ , the variation of  $\mathcal{A}$  between the present and  $z = 5$  is less than 1% for  $|g_{QS}| < 0.5$ .

Next, we consider models in which  $c_g$  varies with time. Here the deviation scale  $k_t$  of the theory can vary significantly with time. As a toy model, let us assume that  $c_g(a)$  depends on the square of the scale factor

$$c_g(a) = c_g(0) \cdot a^2, \quad (20)$$

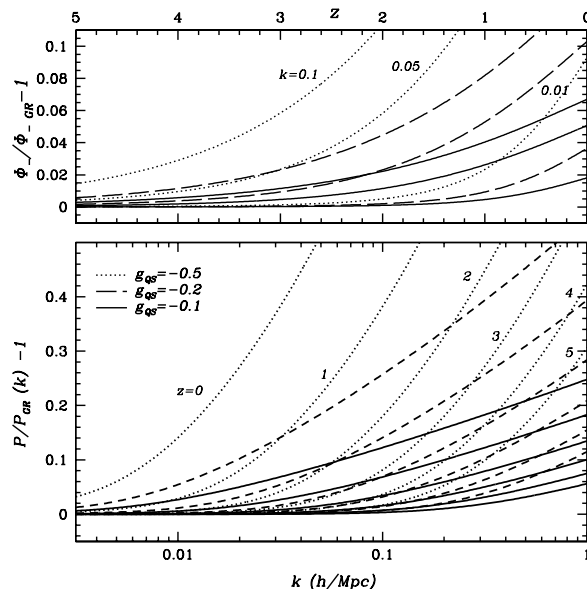


FIG. 4: Deviation of  $\Phi_-$  (upper) and power spectrum  $P(k)$  (lower) compared with GR, assuming  $g(a, k)$  has the form of Eq. (15) and Eq. (20),  $c_g(0) = 0.1$ .

and parametrize the model by the value of  $c_g(0)$ . In this case,  $k_t$  will always decrease, and for a fixed wavenumber the absolute value of the deviation  $|g|$  will always increase with time. Consequently, as illustrated in Fig. (4),  $\Phi_-(k)$  (upper panel) and the power spectrum (lower panel) will deviate from the GR case progressively.

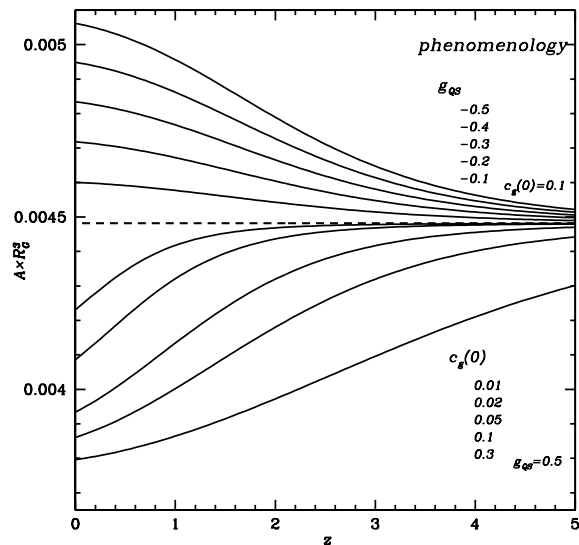


FIG. 5: The redshift evolution of genus amplitude for phenomenological models described by Eq.(15) and Eq.(20). The upper panel shows models with different  $g_{QS}$  while keeping  $c_g(0) = 0.1$ . The lower panel shows models with different different  $c_g(0)$  while keeping  $g_{LS} = 0.5$ . The dashed line corresponds to the GR case in each panel.

In Fig. (5), we can see the evolution of the genus for different model parameters. In the upper panel,  $g_{QS}$  is varied, taking values from  $-0.5$  to  $-0.1$  while  $c_g = 0.1$ . As expected, for the cases with larger value of  $g_{QS}$ , the genus amplitude take a faster raise. In the lower panel, We show the result of varying the value of  $c_g(0)$ , while keeping  $g_{LS} = 0.5$  fixed. In this case, increase  $c_g(0)$  would move  $k_t$  to larger scales, and shift the onset of the deviation to an earlier epoch, so the genus should deviate from GR further and earlier. However, when  $c_g(0) \gtrsim \mathcal{O}(1)$ , the modification

TABLE I: Parameters of future large scale structure surveys.

Galaxies Survey	redshift range	sky area
BOSS	$0.2 < z < 0.7$ ,	10000 deg <sup>2</sup>
LAMOST	$0.0 < z < 0.7$ ,	8000 deg <sup>2</sup>
WF MOS	$0.5 < z < 1.3$ ,	2000 deg <sup>2</sup>
JDEM	$0.5 < z < 2.0$ ,	10000 deg <sup>2</sup>
BIGBOSS	$0.2 < z < 2.0$ ,	24000 deg <sup>2</sup>

21cm Intensity Mapping	redshift range	other parameter	integration time (hour)
MWA	$3.5 < z < 5$ ,	$N_a = 500, A_s = 16\pi^2$ deg <sup>2</sup>	1000
MWA5000	$3.5 < z < 5$ ,	$N_a = 5000, A_s = 16\pi^2$ deg <sup>2</sup>	4000
CRT	$0 < z < 2.5$ ,	$L = 100m, W = 15m \times 7$ ,	10000

would move to superhorizon regime, then it would become saturated with a nearly constant genus.

#### IV. PROSPECTS OF OBSERVATION

The genus curve of iso-density contours could be measured with future large scale structure surveys. In the following, we consider how such surveys could be used to constrain the modified gravity models with the topological measurements discussed above.

The variance of the genus measurement is usually estimated with the help of simulation. In principle, the uncertainty in the topological measurement is different from the uncertainty in the power spectrum of the large scale structure. This is especially true for the general (non-gaussian) case. However, as a simple estimate, we may approximately calculate the minimal amount of statistical uncertainty  $\sigma_{\mathcal{A}}$  by propagating from the uncertainty of the power spectrum  $\sigma_P(k)$ . The details of the calculation is given in the appendix.

Throughout this section, we assume the Gaussian smoothing scale  $R_G = 15\text{Mpc}/h$  unless explicitly emphasized otherwise. At high redshifts the non-linear scale decreases, one can use smaller  $R_G$  which makes the uncertainty of the genus much smaller.

Taking  $\mathcal{O} = \ln \mathcal{A}$  as the observable, the Fisher matrix is

$$F_{ij} = \sum_{\text{redshift bins}} \frac{\partial \mathcal{O}}{\partial p_i} \frac{1}{\sigma_{\mathcal{O}}^2} \frac{\partial \mathcal{O}}{\partial p_j} + F_{\text{CMB}, ij}, \quad (21)$$

where  $p_i$  include  $\Omega_m h^2, \Omega_b h^2, h_0, n_s, \ln A_s, \tau, w_e$ , as well as other modified gravity parameters, e.g.  $B_0$  for  $f(\mathcal{R})$  theory. The Planck prior is added effectively by the contribution  $F_{\text{CMB}}$ , which helps to break the degeneracies between the various parameters. The summation is over different redshift bins with size of  $\Delta z = 0.1$ . For cosmological parameters ( $\Omega_m h^2, h_0, w_e$ ), both the perturbations and background evolution contribute to the constraints. Therefore, derivatives in Eq.(21) should be carefully calculated by taking into account the scaling relation

$$\mathcal{A}_{\text{obs}}(R_G) = \lambda \mathcal{A}_{\text{true}}(\lambda^{1/3} R_G) \quad (22)$$

$$\lambda(z) = \frac{D_{\text{A,ref}}^2 H}{D_{\text{A}}^2 H_{\text{ref}}}. \quad (23)$$

Here  $D_{\text{A,ref}}$  and  $H_{\text{ref}}$  are the angular diameter distance and the Hubble expansion rate evaluated in the reference cosmology, which is used when reconstructing the position from redshift, and for simplicity we assumed it as the same as the fiducial cosmology.

We consider the measurement of large scale structure topology in extended redshift ranges with a number of optical/near IR galaxy surveys at  $z < 2$ , such as the LAMOST<sup>2</sup> (see also [40]), BOSS<sup>3</sup>, WF MOS[41], JDEM<sup>4</sup> and

<sup>2</sup> <http://www.lamost.org/>

<sup>3</sup> <http://cosmology.lbl.gov/BOSS/>, <http://www.sdss3.org/>

<sup>4</sup> <http://www.jdem.gsfc.nasa.gov/>

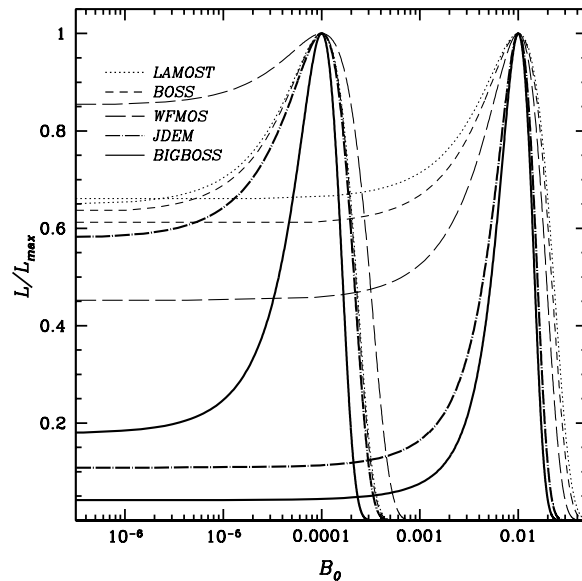


FIG. 6: Likelihood distribution on  $B_0$  of  $f(\mathcal{R})$  theory for various optical/IR surveys. Two fiducial value ( $B_0 = 0.01$  and  $0.0001$ ) are shown in the figure.

BIGBOSS[42] survey, as well as a few 21cm intensity mapping experiments at  $0 < z < 5$ , e.g. the CRT[43, 44] and the MWA<sup>5</sup>. The survey parameters we adopt are listed in Table (I). Note that these are only preliminary estimates, the actual case may be quite different.

In Fig. (6), we illustrate the likelihood distribution over  $B_0$  of the  $f(\mathcal{R})$  theory at fiducial values  $B_0 = 10^{-2}$  and  $10^{-4}$  calculated for various galaxies surveys. As one of the projects under planning, the BIGBOSS can provide the most stringent constraints, the  $1-\sigma$  error on  $B_0$  is 0.0039 at  $B_0 = 10^{-2}$  and  $5.38 \times 10^{-5}$  at  $B_0 = 10^{-4}$ . Even for surveys which are on going or will start in the near future (e.g. BOSS and LAMOST), one could also gain considerably rich information about the redshift evolution of the genus amplitude. The  $1-\sigma$  errors at the same fiducial values are 0.011 and  $1.1 \times 10^{-4}$  for LAMOST, 0.010 and  $1.04 \times 10^{-4}$  for BOSS respectively. Notably, the constraining conclusion drawn from particular survey depends on the true cosmology, not only quantitatively but also qualitatively. For example, the WFMOS survey, which is deep but narrow and is more powerful than BOSS and LAMOST survey at  $B_0 = 10^{-2}$ , become insignificant at  $B_0 = 10^{-4}$ . This is because when  $B_0$  is small, the amplitude of genus at high redshift would quickly approach to the value of GR (c.f. Fig. 2) and become nearly indistinguishable for a narrow survey.

Unlike galaxies surveys, the 21cm intensity mapping experiments have relatively poor angular resolutions, for the CRT

$$R_{\text{res}}(z) = r(z) \frac{\lambda}{L_{\text{CRT}}} \quad (24)$$

can reach to the order of  $10 \sim 30 \text{Mpc}/h$  at higher redshift. Here,  $r(z)$  is the comoving angular diameter distance at redshift  $z$ ,  $\lambda$  is the received wavelength and  $L_{\text{CRT}}$  is the length of the cylinder of the CRT telescope. Therefore the smoothing scale  $R_{\mathcal{G}}$  when measuring the genus should be larger than  $R_{\text{res}}$ .

We plot in Fig. (7) the likelihood of  $B_0$  for the 21cm intensity mapping. For the CRT, two different choices of  $R_{\mathcal{G}}$  are considered here. One is the constant  $R_{\mathcal{G}}$  model by assuming  $R_{\mathcal{G}} = 2 \times \max\{R_{\text{res}}(z)\}$ , which equals to  $60 \text{Mpc}/h$  in this case. The figure shows that the constraint of this model is not very stringent for the  $f(\mathcal{R})$  model. Another choice is to smooth the data with varying  $R_{\mathcal{G}}$  at different redshifts. We divide the whole redshift range ( $0 < z < 2.5$ ) into 4 intervals, and assume the same factor of two relationship between the smoothing scale and the angular resolution within each redshift interval. In this case, the  $1-\sigma$  error equals to 0.0060 at  $B_0 = 10^{-2}$  and  $6.93 \times 10^{-5}$  at  $B_0 = 10^{-4}$ . On the other hand, the angular resolution of the MWA and MWA5000 is sufficiently good so that we assume the same smoothing scale as the optical/IR case. However, for their high redshift coverage, the constraints are still not very stringent, especially at  $B_0 = 10^{-4}$ .

<sup>5</sup> <http://www.MWAtlescope.org/>

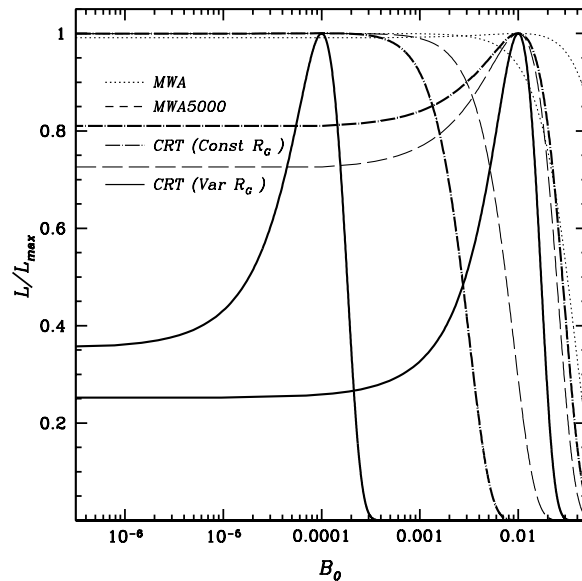


FIG. 7: The same plot as Fig.(6) for 21cm surveys.

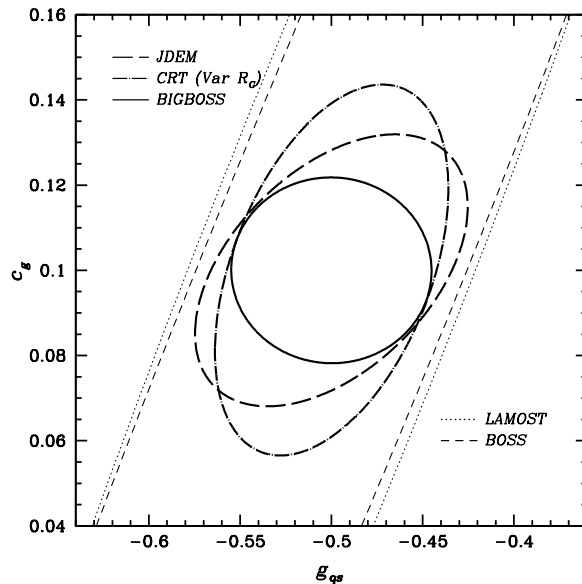


FIG. 8: 1- $\sigma$  constraint on  $g_{QS}$  and  $c_g(0)$ , assuming  $c_g(a) = c_g(0) \cdot a^2$

In Fig. (8), we also plot the 2D constraint on  $g_{QS}$ - $c_g(0)$  for the phenomenological model considered in Eq. (15,20). Similar to the case of  $f(\mathcal{R})$  model, the BIGBOSS provides a very stringent constraint, the 1- $\sigma$  errors are  $\sigma_{g_{QS}} = 0.036$  and  $\sigma_{c_g(0)} = 0.014$  respectively. For the CRT,  $\sigma_{g_{QS}} = 0.042$  and  $\sigma_{c_g(0)} = 0.028$  (assume the redshift-varying  $R_G$ ).  $\sigma_{g_{QS}} = 0.18$  and  $\sigma_{c_g(0)} = 0.19$  for the LAMOST, and  $\sigma_{g_{QS}} = 0.17$  and  $\sigma_{c_g(0)} = 0.18$  for the BOSS.

## V. CONCLUSION

The topological indicators such as the genus of the isodensity contours provides an independent way for characterizing the large scale structure, complementary to the more often used two point statistics such as the correlation function and power spectrum. A significant advantage of the the topological measurement is that it is less susceptible

to the non-linear evolution and bias of the large scale structure, thus reducing the effects of these potential systematic errors, and may therefore be a more reliable way to extract the information on the large scale structure.

In this paper, we studied the topology of the large scale structure as a measure of the scale-dependent expansion history of the universe in models of modified gravity theories. In the modified gravity theory models, the structure growth can be scale-dependent even in the linear regime, the amplitude of the genus curve varies significantly with redshift, and hence it can be used as a new tool for distinguishing the models from the case of standard gravity (i.e. GR). We illustrated this for the  $f(\mathcal{R})$  theory, DGP braneworld model as well as a phenomenological model parametrized with the PPF variables introduced by [32]. We find that the genus curves for these models are modified and evolve with redshift due to the scale-dependent growth effect, hence the genus curve can be used as an observable to distinguish the modified gravity models from the general relativity theory. Finally, using the Fisher matrix formalism, we also made forecast on the sensitivity of this test with some current or future optical/IR and 21cm redshift surveys, showing that the method is a competitive way to test modified gravity models.

### Acknowledgements

This work is supported by the National Science Foundation of China under the Distinguished Young Scholar Grant 10525314; by the Chinese Academy of Sciences under grant KJCX3-SYW-N2; by the Ministry of Science and Technology of China under the National Basic Science program (project 973) grant 2007CB815401; and by the National Research Foundation of Korea (NRF) grant funded by the Korea government MEST (No. 2009-0062868)

### Appendix: Statistical Uncertainty of the Genus Measurement

Since the genus amplitude  $\mathcal{A}$  can be expressed as a function of the power spectrum (Eq. 2), we may approximately estimate the statistical uncertainty  $\sigma_{\mathcal{A}}$  by propagating the error from the uncertainty of power spectrum  $\sigma_P(k)$ .

Rewriting the observable

$$\mathcal{O} = \ln(\mathcal{A}) = (3/2)[\ln(\mathcal{M}_4) - \ln(\mathcal{M}_2)],$$

where  $\mathcal{M}_n$  is defined as

$$\mathcal{M}_n = \int d^3k k^{n-2} P_X(\vec{k}) W(kR_G), \quad (25)$$

$P_X(\vec{k})$  denotes the power spectrum under consideration, then the variance  $\sigma_{\mathcal{O}}^2 \equiv \text{Var}(\mathcal{O})$  is simply

$$\sigma_{\mathcal{O}}^2 = \left(\frac{3}{2}\right)^2 \left[ \frac{\text{Var}(\mathcal{M}_2)}{\mathcal{M}_2^2} + \frac{\text{Var}(\mathcal{M}_4)}{\mathcal{M}_4^2} - 2 \frac{\text{Cov}(\mathcal{M}_2, \mathcal{M}_4)}{\mathcal{M}_2 \mathcal{M}_4} \right]. \quad (26)$$

Here  $\text{Var}(\mathcal{M}_m) \equiv \text{Cov}(\mathcal{M}_m, \mathcal{M}_m)$ , and  $\text{Cov}(\mathcal{M}_m, \mathcal{M}_n)$  is propagated from  $\sigma_P^2$

$$\text{Cov}(\mathcal{M}_m, \mathcal{M}_n) = \langle \mathcal{M}_m \mathcal{M}_n \rangle - \langle \mathcal{M}_m \rangle \langle \mathcal{M}_n \rangle = \frac{2(2\pi)^2}{V_s} \int dk d\mu k^{(m+n-2)} W^2(kR_G) \sigma_{P_X}^2(\vec{k}). \quad (27)$$

where  $\mu$  is the cosine of the angle between  $\vec{k}$  and the line of sight,  $V_s$  is the survey volume. We have assumed the covariance matrix of power spectrum is diagonal,

$$\text{Cov}(P(\vec{k}_1), P(\vec{k}_2)) = \delta_D(\vec{k}_1 - \vec{k}_2) \frac{2(2\pi)^2}{V_s} \sigma_{P_X}^2 \quad (28)$$

We need to estimate the statistical uncertainty in power spectrum measurements for the different experiments. For galaxy surveys, the statistical uncertainty of  $P_g(k)$  per Fourier mode includes both the cosmic variance and the shot noise due to the finite number of galaxies:

$$\sigma_{P_g}(\vec{k}) = \left[ P_g + \frac{1}{n} \right], \quad (29)$$

As is often done in such estimates (e.g. [45]), we assume the density of the galaxy  $n(z)$  satisfies  $nP(k=0.2) = 3$ .

For the 21cm intensity mapping experiment, e.g. the cylindrical radio telescope (CRT), in addition to the cosmic variance and the shot noise due to the finite number of galaxies, there is also the noise due to the foreground and receiver [44], so  $\sigma_{P_{21cm}}(\vec{k}) = P_{21cm}(\vec{k})$ , with

$$P_{21cm}(\vec{k}) = p_s^2 \left( P_{HI}(\vec{k}) + \frac{1}{n} \right) + \left( \frac{k_B(g\bar{T}_{\text{sky}} + \bar{T}_a)\Delta f}{\sqrt{t_{\text{int}}\Delta f}} \right)^2 V_R \quad (30)$$

with  $p_s = k_B g \bar{T}_{\text{sig}} \Delta f$ ,  $g = 0.8$  is the gain,  $t_{\text{int}}$  is the integration time and  $V_R$  is the volume of a pixel,  $\bar{T}_{\text{sig}}$  is the average brightness temperature which is estimated as

$$\bar{T}_{\text{sig}} = 188 \frac{x_{HI}(z)\Omega_{H,0}h(1+z)^2}{H(z)/H_0} \text{mK}, \quad (31)$$

with a conservative assumption for the neutral hydrogen fraction  $x_{HI}(z)\Omega_{H,0} = 0.00037$ .  $\bar{T}_{\text{sky}}$  and  $\bar{T}_a$  are average sky and antenna noise temperatures, which are assumed to equal to 10K and 50K respectively.

For the high redshift 21cm experiment such as the MWA, we assume that the system temperature of the telescope is dominated by the sky:

$$\bar{T}_{\text{sys}} \sim 250[(1+z)/7]^{2.6} \text{K},$$

and the observation time is

$$t_k = (A_e t_{\text{int}} / \lambda^2) n(k_{\perp})$$

at  $k_{\perp}$ , where  $n(k_{\perp})$  is the number of baselines which observe the transverse component of the wavevector. This can be calculated from the array configuration, here we model the antennas distribution of MWA as  $\rho(r) \sim r^{-2}$ , with radius  $r_m = 750\text{m}$  and a flat core of radius  $r_c = 20\text{m}$ . For the hypothetical follow-up of MWA, denoted as MWA5000, we have assumed  $r_m = 2\text{km}$  and  $r_c = 80\text{m}$ .

The results of our estimates are given in Sec.4.

- 
- [1] Tegmark, M., et al., 2006, PRD, 74, 123507.
  - [2] Percival, W. J., et al., 2007, MNRAS, 381, 1053.
  - [3] Gaztanaga, E., Cabre, A., Hui, L., 2009, MNRAS, 399, 1663
  - [4] Kim, J., Park, C., Gott, J. R., Dubinski, J., 2009, ApJ, 701, 1547
  - [5] Crocce, M., Scoccimarro, R., 2006, PRD, 73, 063519.
  - [6] Crocce, M., Scoccimarro, R., 2006, PRD, 73, 063520.
  - [7] Crocce, M., Scoccimarro, R., 2008, PRD, 77, 023533.
  - [8] Matsubara, T., 2008, Phys. Rev. D 77, 063530
  - [9] Matsubara, T., 2008, Phys. Rev. D 78, 083519
  - [10] Smith, R. E., Scoccimarro, R., Sheth, R. K., 2007, PRD, 75, 063512
  - [11] Padmanabhan, N., White, M., Cohn, J. D., 2009, PRD, 79, 3523
  - [12] Noh, Y., White, M., Padmanabhan, N., 2009, PRD, 80, 3501
  - [13] Park, C., Kim, J., & Gott, J. R., 2005, ApJ, 633, 1.
  - [14] Park, C., Kim, Y. R., 2010, ApJ, 715, L185
  - [15] Park, C., 2010, in preparation.
  - [16] Matsubara, T., 1994, ApJ, 434, L43
  - [17] Capozziello, S., Carloni, S., Troisi, A., 2003, Recent Res. Dev. Astron. Astrophys., 1. 625
  - [18] Carroll, S. M., Duvvuri, V., Trodden, M., Turner, M. S., 2004, PRD, 70, 043528
  - [19] Nojiri, S., Odintsov, S. D., 2003, PRD, 68, 123512
  - [20] Song, Y.-S.; Hu, W.; Sawicki, I., 2007, PRD., 75, 044004.
  - [21] Dvali, G. R., Gabadadze, G., Porrati, M., 2000, Phys. Lett. B, 485. 208
  - [22] Linder, E. V., 2005, PRD, 72. 043529
  - [23] Zhang, P., Liguori, M., Bean, R., Dodelson, S., 2007, PRL, 99. 141302
  - [24] Khoury, J. & Weltman, A., 2004, PRL, 93, 171104.
  - [25] Khoury, J. & Weltman, A., 2004, PRD, 69, 044026.
  - [26] Vainshtein, A. I, 1972, PLB, 39, 393.
  - [27] Deffayet, C., Dvali, G., Gabadadze, G., Vainshtein, A. 2002, PRD, 65, 044026.
  - [28] Huterer, D. Linder, E. V., 2007, PRD, 75. 023519
  - [29] Doroshkevich, G., 1970, Astrophysika, 6, 320

- [30] Hamilton, A. J. S., Gott, J. R., Weinberg, D., 1986, ApJ, 309. 1H
- [31] Matsubara, T., 2003, ApJ584, 1.
- [32] Hu, W. and Sawicki, I., 2007, PRD, 76, 104043
- [33] Fang, W., Hu, W., Lewis, A., 2008, PRD., 78, 087303
- [34] Fang, W. et. al, 2008, PRD., 78, 103509
- [35] Lewis, A. & Bridle, S., 2002, PRD, 66, 103511.
- [36] Sawicki, Ignacy; Song, Yong-Seon; Hu. Wayne; 2007, PRD, 75, 4002
- [37] Chan., K., C., & Scoccimarro, R., 2009, PRD, 80, 104005
- [38] Scoccimarro, R., 2009, PRD, 80, 104006
- [39] Hu, W., 2008, PRD, 77,103524
- [40] Wang, X., et al., 2009, MNRAS, 394, 1175
- [41] Bassett, B. A., Nichol, R. C., Eisenstein, D. J., 2005, A&G., 46, 26.
- [42] Schlegel, David J., et al. arXiv:0904.0468
- [43] Chang, T. C., Pen, U. L., Peterson, J. B., and McDonald, P., 2008, PRL, 100. 091303
- [44] Seo, Hee-Jong, et al., 2009, arXiv:0910.5007
- [45] Seo, H. J. & Eisenstein, D. J., 2003, ApJ 598, 720.